Propagation characteristics control by variation of PCF structural parameters

James F Jena[1], Peter Baricholo[1], Temba S Dlodlo[1] and Paul K Buah-Bassuah[2]

[1]Department of Applied Physics, National University of Science and Technology, P.O.Box AC939, Ascot, Bulawayo, Zimbabwe
[2]Department of Physics, University of Cape Coast, Cape Coast, Ghana

james.jena@nust.ac.zw, effjay.jena@gmail.com

Abstract. A photonic crystal slab was designed in COMSOL Multiphysics using gallium arsenide (GaAs) pillars placed equidistant from each other in air. A defect was created by removing some GaAs pillars across the crystal slab geometry to form a 90^o bend through the structure. Structural parameters; the pillar diameter and inter-pillar spacing were separately varied and waves were propagated through the created defect with different allowed wavelengths, within and determined by the photonic crystal's bandgap. It was observed for the air filling fraction at constant pitch that, when the factor given by the ratio of the air hole diameter to the pitch is less than 0.63, an increase in air hole diameter requires corresponding increase in the wavelength which can be propagated within the waveguide with minimum loss. When both air hole diameter and pitch were varied the increase in the air filling fraction was also observed to result in a photonic bandgap of lower frequency range as only larger wavelengths would be allowed to propagate. When the air filling fraction factor was less than 0.63 the photonic crystal waveguides exhibited slightly increased confinement and bend loss. The diameter and pitch affected the core resonance resulting in selected wavelength bands being propagated through the created defect in the waveguide. Only those bands whose value coincides with the photonic bandgap were allowed to propagate.

1. Introduction

Photonic crystals are materials of periodic dielectric media which are able to localise light in specific areas and prevent it from propagating in certain directions. Their structural build up resembles the lattice structures of crystalline materials and they have photonic bandgaps whose optical properties are analogous to the energy bandgaps [1] in electrical semiconductors. Light propagation in a hollow core is possible within photonic crystal fibers (PCFs). These are single material optical waveguides with an array of periodic air holes across the transverse section running down their entire length. In the cladding, the refractive index is modulated in space on a wavelength scale [2]. Very high powers can be propagated without being limited by material threshold [3]. PCFs have application in supercontinuum generation, optical coherence tomography, frequency metrology, microscopy and spectroscopy [4]. Many modelling techniques have been applied to study propagation characteristics [5] of solid core, index guiding PCF's. For hollow core PCF's the control of propagation characteristics which include dispersion, bend loss, confinement loss and effective index are determined by the structural parameters, namely air hole diameter and the pitch. Through simulation, COMSOL Multiphysics [6], a finite element method based software, was used to design and study various photonic crystal structures distinguished by variation in structural parameters and their associated wave propagation characteristics. Confinement loss, bend loss and the allowed photonic bandgap wavelength were monitored for the various air filling fractions.

2. Theory and Simulation Design

In a photonic crystal with periodic dielectric medium of periodicity (Λ), any wave of wavelength comparable to twice the periodicity [7] is not allowed to propagate through the photonic crystal. The wave is within the photonic bandgap, hence it is highly reflected. The partial reflections at each period

are in phase. As they reinforce one another, they form standing waves [8] with the incident wave and as a result such a wave will not be propagated. The other waves with a frequency outside the bandgap experience no scattering as the periodic variation in the refractive index results in the scattering cancelling out coherently [7], so they propagate with minimal attenuation. When a hollow line defect is created in such media the reflecting wave can be allowed to propagate within the defect and the crystal material becomes a waveguide. Varying the periodicity by altering the inter-hole spacing or the air hole diameter affects the wavelength that can be guided as well as the propagation characteristics. Photonic crystal slabs were designed in COMSOL Multiphysics [6] using GaAs pillars placed equidistant from each other in air. A line defect was created by removing some GaAs pillars to form a 90^{o} bend across the slab geometry as shown in figure 1. The structure is a square lattice [9] which has a simpler arrangement than the triangular and hexagonal lattice structures. The bend was chosen to determine with certainty that the defect has guidance to the propagating wave while this motivated study of the effects of structural parameter variation on bend loss.

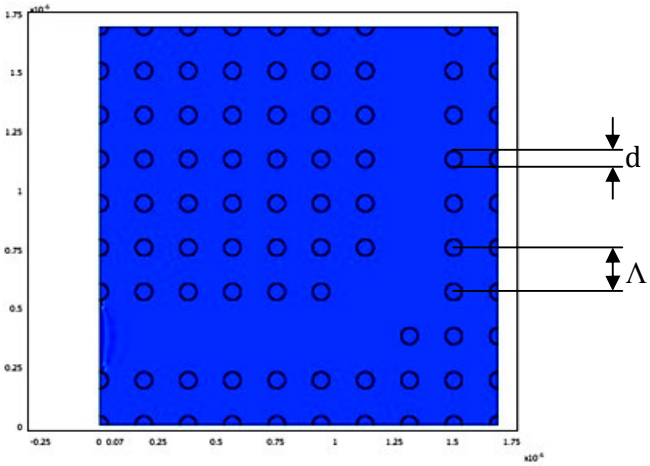

Figure 1. A 2D photonic crystal slab with a 90º bend across its geometry.
(pillar diameter, $\mathrm{d} = 0.7 \times 10^{-7}\mathrm{m}$ and pitch, $\Lambda = 1.875 \times 10^{-7}\,\mathrm{m}$).

As determined by the photonic bandgap, different allowed wavelengths within the photonic crystal's bandgap are found and the waves propagated along the 90º bend in different slabs of varying pillar diameter and pitch. The air filling fraction factor (f) given by the ratio in (1) is calculated for each design [10] using this relation;

$$f = (\Lambda - \mathrm{d})/\Lambda \qquad (1)$$

where Λ is the pitch given by the inter-pillar spacing and d is the GaAs pillar diameter. $(\Lambda - \mathrm{d})$ represents the air gap separating any adjacent pillars. Low-reflecting boundaries were used on all external boundaries by setting them to the scattering boundary condition and the source at the input set as a plane wave whose electric field in the z component has unit initial amplitude($\mathrm{E_z} = 1\ \mathrm{Vm^{-1}}$).

3. Simulation

The pitch was maintained constant at $3.75 \times 10^{-7}\mathrm{m}$ and the pillar diameter varied within the range $0.7 \times 10^{-7}\mathrm{m}$ to $2.8 \times 10^{-7}\mathrm{m}$. Results were recorded for the guided wavelength (λ) and the corresponding air filling fraction. The pitch was then varied from $1.875 \times 10^{-7}\,\mathrm{m}$ to $7.5 \times 10^{-7}\,\mathrm{m}$ while the diameter remained constant at $1.4 \times 10^{-7}\,\mathrm{m}$. The values obtained were used to make plots of normalised wavelength against air filling fraction. Bend loss was determined from measurement of the amplitude of the electric field after the 90º bend through the use of a scaled profile from the cross

sectional plot function. Confinement loss was determined qualitatively from examination of the 3D propagation plots in which modes were seen to leak away from the defect through the boundaries into the photonic crystal. Simulation designs were altered through variation of photonic crystal structural parameters. The same square lattice structure was maintained through all designs as shown in figures 2a and 2b.

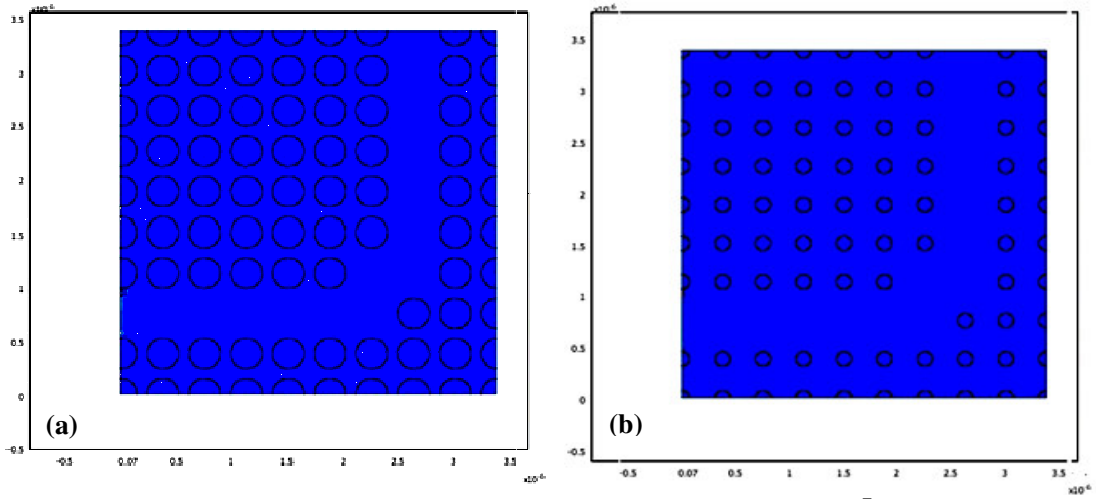

Figure 2. 2D Photonic crystal slabs with same value of pitch $\Lambda = 3.75 \times 10^{-7}$m. **(a)** $d = 2.8 \times 10^{-7}$m, $f = 0.63$ **(b)** $d = 1.4 \times 10^{-7}$m, $f = 0.25$

4. Simulation Results and Analysis

Three dimensional views of the wave propagation through the photonic crystal slabs are presented in figures 3, 4 and 5. The guided wavelengths were recorded. A difference in propagation is notably distinguishable in variable designs while identical designs show similar propagation characteristics, only at different wavelengths (figure 5d). The diameter was varied and the air filling fraction factor (f) calculated while pitch was maintained constant at a chosen standard value of $\Lambda_s = 3.75 \times 10^{-7}$m.

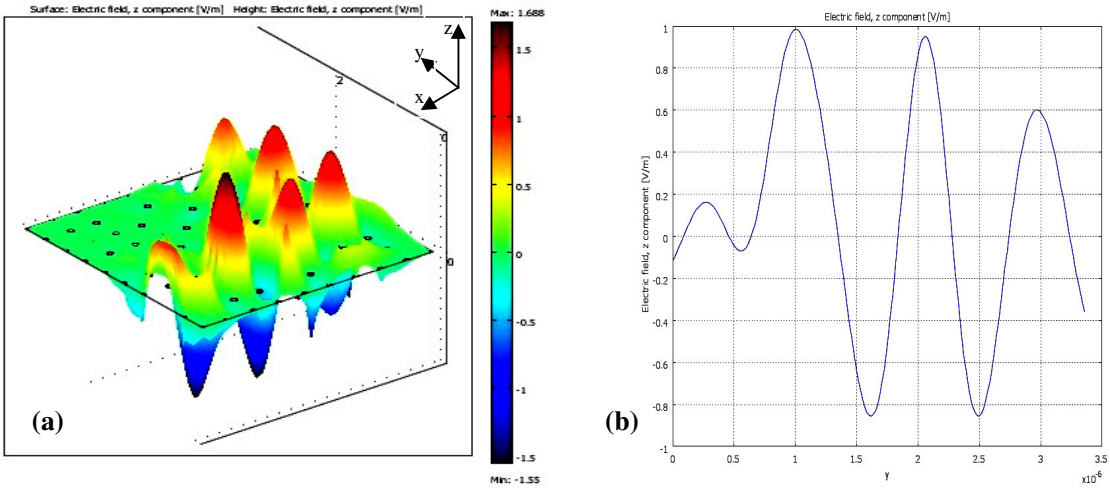

Figure 3. Simulation results for constant pitch $\Lambda_s = 3.75 \times 10^{-7}$m: **(a)** 3D propagation for $d = 0.7 \times 10^{-7}$m, $f = 0.81$, $\lambda = 7.8 \times 10^{-7}$m . **(b)** z-y Cross sectional plot of Electric field (E_z) in figure 3a, after the 90^0 bend, $E_z = 0.98\ \mathrm{Vm}^{-1}$.

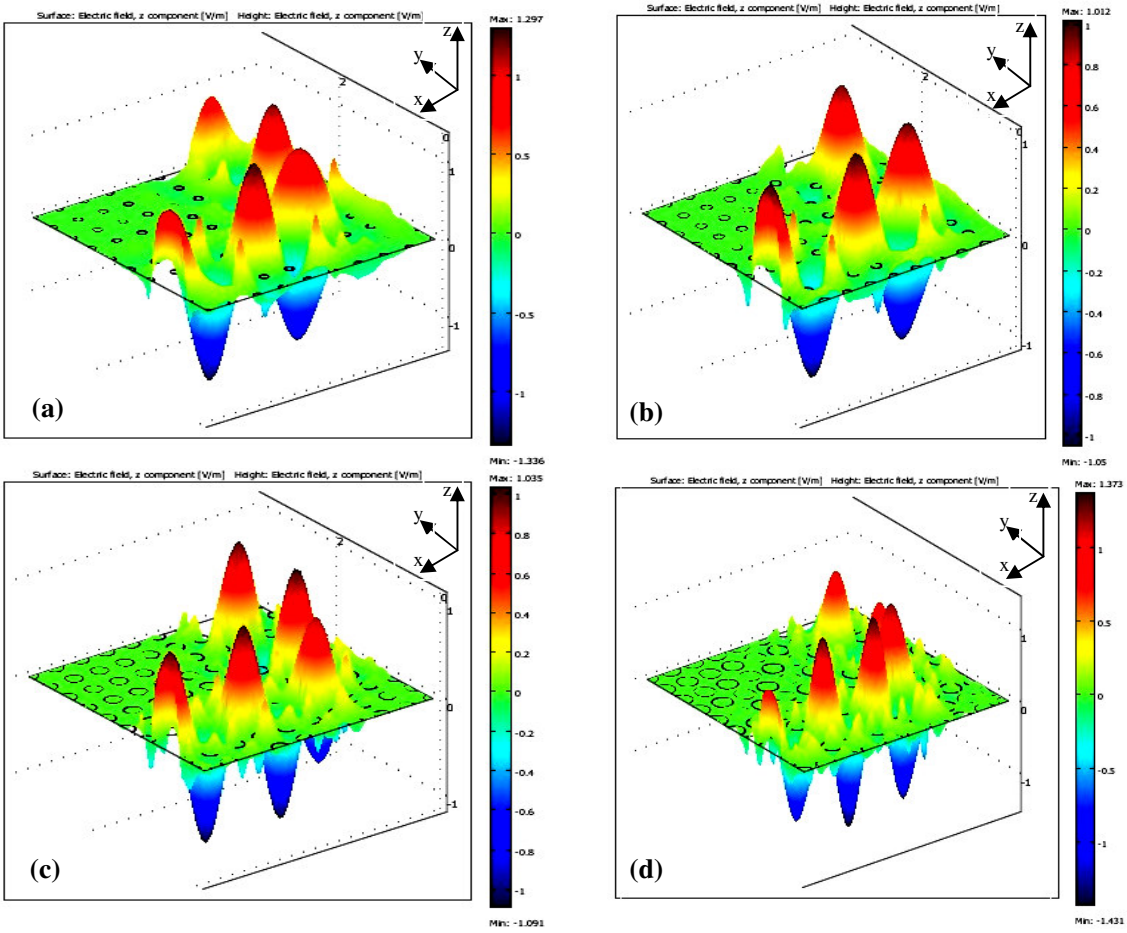

Figure 4. Simulation results for 3D propagation at constant pitch Λ_s: **(a)** $d = 1.05 \times 10^{-7}\text{m}, f = 0.72, \lambda = 9.3 \times 10^{-7}\text{m}$ $E_z = 1.00\ \text{Vm}^{-1}$. **(b)** $d = 1.4 \times 10^{-7}\text{m}, f = 0.63, \lambda = 1.0 \times 10^{-6}\text{m}$ $E_z = 0.60\ \text{Vm}^{-1}$ **(c)** $d = 2.1 \times 10^{-7}\text{m}, f = 0.44, \lambda = 7.98 \times 10^{-7}\text{m}$ $E_z = 0.90\ \text{Vm}^{-1}$. **(d)** $d = 2.8 \times 10^{-7}\text{m}, f = 0.25, \lambda = 6.8 \times 10^{-7}\text{m}$ $E_z = 0.55\ \text{Vm}^{-1}$.

In figure 3b, the cross sectional plot is used to determine the electric field amplitude ($E_z = 0.98\text{Vm}^{-1}$) of figure 3a, after the bend. The photonic crystal introduces evanescence to waves whose frequencies are below the bandgap cut-off (figure 5c) while for higher frequencies outside the bandgap it is transparent and incoherently scattering. When compared to figures 4a and 4b, figures 4c, 4d, 5a and 5b show that the smaller wavelengths seem to propagate with increased confinement loss, as they tend to leak away into the cladding. Confinement loss is significant for small air filling fractions [11], where $f < 0.625$ while bend loss is slightly higher for air filling fractions between $0.25 < f < 0.5$ and $0.63 < f < 0.72$ as deduced from the electric field amplitude values of figures 3, 4 and 5. Figure 6b shows that varying the pitch at constant pillar diameter has the effect of decreasing the bandgap frequency with increasing air filling fraction. Larger wavelengths are accommodated as the air holes separating the pillars are increased and so is the air filling fraction (figures 4a and 4b). In figure 5d, when the air filling fraction is the same for similar structural geometry but having proportionately different structural parameter dimensions then the permitted wavelength varies directly as the air hole spacing as evidence in figures 4d and 5a.

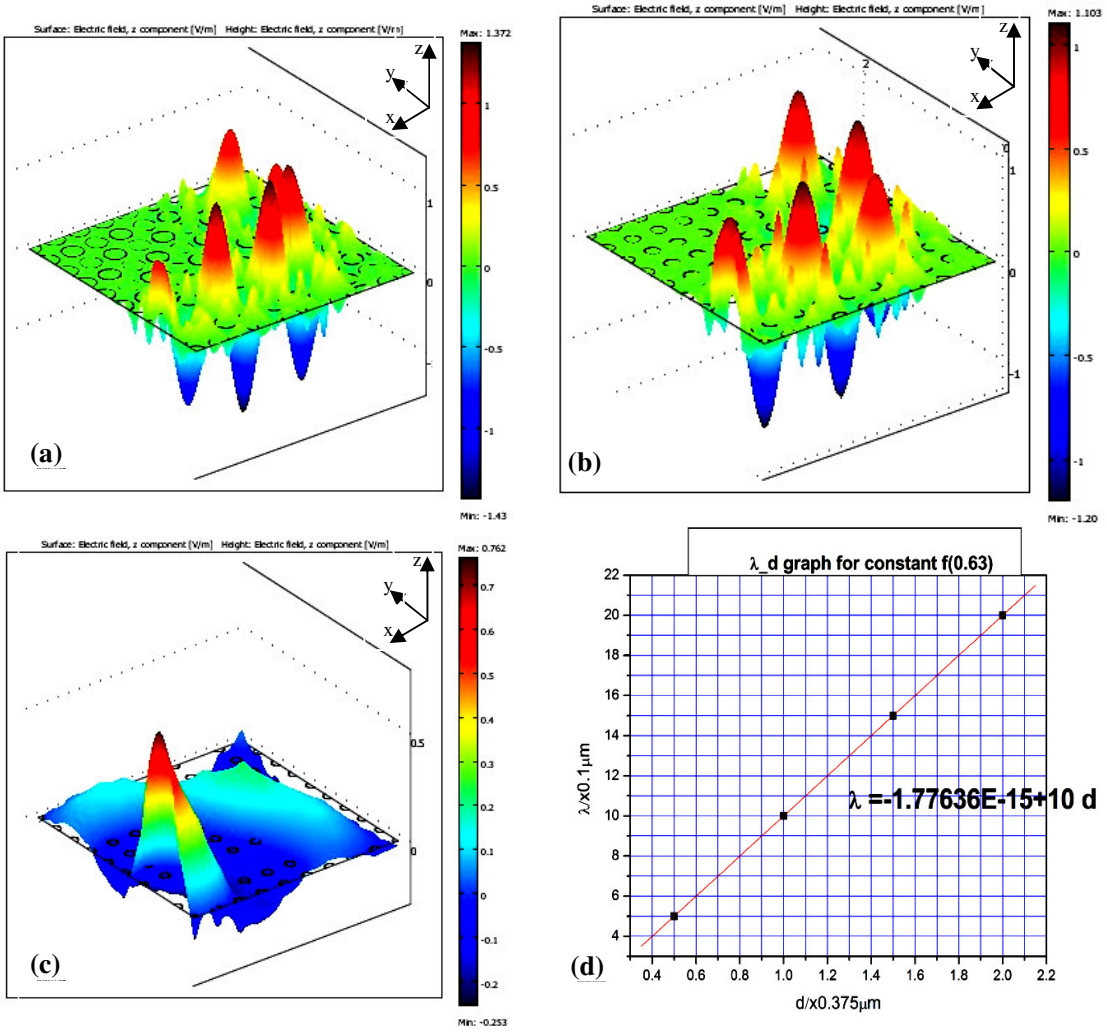

Figure 5. Simulation results for propagation of different wavelengths through the photonic crystal: **(a)** 3D propagation with pillar diameter constant at $d = 1.4 \times 10^{-7}\text{m}, f = 0.25, \Lambda = 1.875 \times 10^{-7}\text{m}, \lambda = 3.39 \times 10^{-7}\text{m}$ $E_z = 0.60\ \text{Vm}^{-1}$. **(b)** $d = 1.4 \times 10^{-7}\text{m}, f = 0.5, \Lambda = 2.81 \times 10^{-7}\text{m}, \lambda = 5.82 \times 10^{-7}\text{m}$ $E_z = 1.00\ \text{Vm}^{-1}$. **(c)** Evanescence when optical frequency is not within the bandgap $d = 0.7 \times 10^{-7}\text{m}, f = 0.63, \Lambda = 1.875 \times 10^{-7}\text{m}, \lambda = 1.0 \times 10^{-6}\text{m}$. **(d)** Variation of wavelength with inter-pillar spacing at constant air filling fraction $f = 0.63$.

The simulation results in figures 3 to 5b were used to obtain values of wavelength and air filling fraction to plot the graphs in figures 5d and 6. Increase in air filling fraction at constant pitch requires corresponding increase in the allowed wavelength until the air filling fraction reaches 0.625. After that further increase in air filling fraction results in a corresponding increase in allowed frequency as opposed to the wavelength [9]. The graph in figure 6a resembles a dispersion curve modelled [4] using the fully vectorial effective index method and the scalar effective index method. A change in the air filling fraction consequently alters the effective index of the crystal [11, 12]. At $f = 0.625$ the wavelength change with refractive index is zero, hence $\lambda/\Lambda = 2.68$ is normalised zero dispersion wavelength.

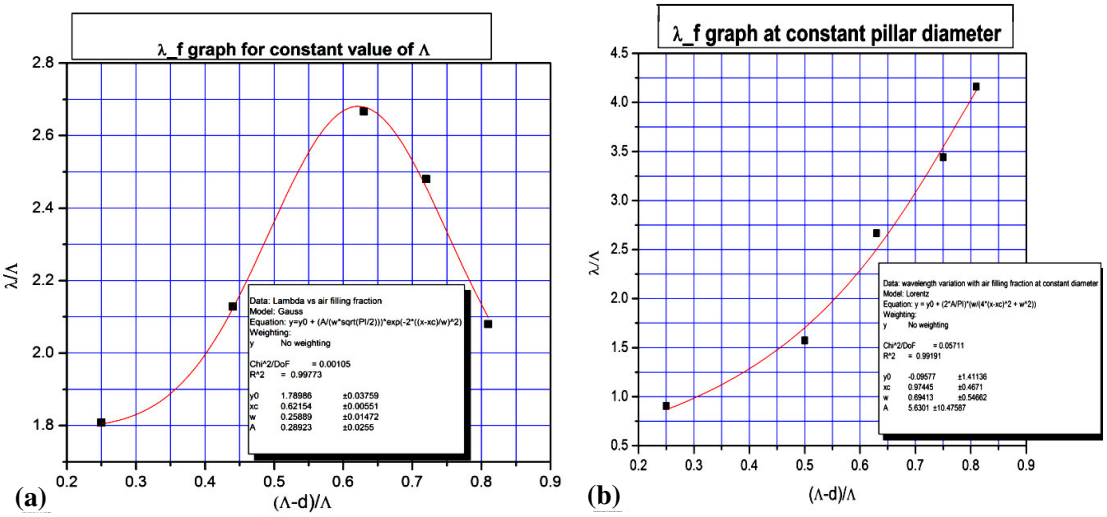

Figure 6. Variation of wavelength with inter-pillar separation: (a) wavelength against air filling fraction determined for constant value of pitch. (b) wavelength against air filling fraction for fixed pillar diameter.

The change in the inverse gradient of figure 6a represents the second derivative of the effective index with respect to wavelength [13, 14]. Similar to the dispersion parameter D, its sign changes from positive to negative as the slope changes from a decreasing to an increasing gradient. This corresponds to the transition from the normal to the anomalous dispersion regime [12].

5. Conclusions

Generally, wavelengths allowed to propagate within the hollow core PCF increase with an increase in the air filling fraction therefore the photonic bandgap is affected by variation of structural parameters. Only frequencies within the bandgap are propagated along the hollow created in the photonic crystal. Confinement loss and bend loss are greater for small air filling fractions. Effective index and dispersion are controlled by variation of air hole diameter and pitch as they are a function of refractive index and wavelength.

Acknowledgements

We thank the National University of Science and Technology for the availing of resources and time with which this research work was carried out and the NUST research board for the funding. We also extend our gratitude to SUPCOM of Tunisia and Prof. Zaghal for availing the software.

References

[1] Stewart D 2005 Photonic Crystal Bandstructures. Cornell Nanoscale Science and Technology Facility

[2] Yablonivitch E 1987 Photonic Band-gap Structures. Phys. Rev. Lett. 58,2059

[3] Khromova I A Melnikov L A 2007 Dispersion Characteristics of hollow – core Photonic Crystal Fibers. T.4 No. 2, 138

[4] Heidt A Hartung B A Bosman G W Krok Patrizia Rohwer E G Schwoerer H and Hartlet B 2011 Coherent Octave Spanning Near-infrared and Visible Supercontinuum Generation in All-normal Dispersion Photonic Crystal Fibers. Opt . Express, Vol. 19, No. 4, 3775

[5] Varshney A D and Ravindra K S 2007 *Propagation characteristicof Photonic Crystal Fiber: Scalar Effective index Method and Fully Vectorial Effective Index Method.* Adv. Studies Theo. Phys. Vol 1, no. 2, 75-78

[6] COMSOL 3.5 2008 COMSOL Multiphysics RF Module Optics and Photonics. CM 010004 COMSOL AB
[7] Johnson S G 2000 Photonic Crystal: Periodic surprises in Electromagnetism.
[8] Srivastan B 2002 Photonic Band Gap Crystals. Rensselaer Polytechnic Institute.
[9] Mohammed M H Jamil M Y and Abdullah A I 2013 Photonic Bandgap Tuning of Photonic Crystals by Air Filling Fraction . Raf. J. Sci. Vol. 24, No. 5, pp 96 – 102.
[10] Pagnoux D Peyrilloux A Roy P Fevrier S Labonte L and Hilaire S 2010 Microstructured Air-Silica Fibres: Recent Developments in Modelling, Manufacturing and Experiment. Institut de Communications Optiques et Microondes
[11] Chen M and Yu R 2005 Confinement losses and optimization in Rectangular-Lattice Photonic crystal Fibers.
[12] Agrawal G P 2001 Nonlinear Optics: *Optics and Photonics*. 3rd Ed. Academic Press, NY.
[13] Ferrando A Silvestre E and Andres P 2001 Designing the Properties of Dispersion – Flattened Photonic Crystal Fibers. Opt. Exp. Vol.9, No. 13, 687.
[14] Ferrando A Silvestre E Miret J J and Andres P 2000 Nearly Zero Ultra – Flattened Dispersion in Photonic Crystal Fibers. Opt. Lett. Vol.25, No. 11.